Zitierweise: Angew. Chem. Int. Ed. 2024, e202319849
doi.org/10.1002/anie.202319849

Immunotherapy

# Ultra-Galactocation to Sialic Acid on Tumor Cells with A Penta-Functional Dendritic Probe for Enhanced Immune-Killing

*Yuhui Yang[+], Yiran Li[+], Caixia Wang, Yuru Wang, Yi Ren, Jie Wu, Huangxian Ju,* and Yunlong Chen**

**Abstract:** Glycans on tumor cell surface have significant impacts in the immune-killing process. Here an ultra-galactocation to sialic acid (Sia) strategy is designed to hugely introduce galactose (Gal) to Sia and on tumor cells in vivo by using a penta-functional dendritic probe (Den@5F), which efficiently enhances the immune-killing of tumor cells. The Den@5F contains five different kinds of functional groups, including Gal, Cy5, amino, phenylboronic acid (PBA) and 4-(4-(hydroxymethyl)-2-methoxy-5-nitrophenoxy) butanoate (mNB), which can be conveniently prepared through a two-step reaction. After injecting into the tumor-bearing mouse, Den@5F can efficiently block Sia through the specific recognition between PBA and Sia on tumor cells and hugely introduce Gal through the subsequent photo-crosslinking between mNB and amino groups to multiply conjugate excessive Den@5Fs. The comprehensively blocked Sia can prevent the immune escape, and the hugely introduced Gal can promote the immune stimulation of the immune cells, which lead to an efficient enhancement of the immune-killing. The proposed strategy provides a significant and promising tool to promote the clinical immunotherapy of tumor.

Glycans on tumor cells mediate a large number of physiological and pathological processes,[1] especially the immune recognition and immune stimulation,[2–4] which are critical to the immune-killing of tumor cells. The functions of these glycans can be divided into two categories, the enhanced stimulation of immune cells and the resisted recognition of tumor cells. The former is mainly contributed by the galactose (Gal) or fucose (Fuc) terminated glycoconjugates,[5–7] while the latter to normally contributed by sialic acids (Sia) terminated glycoconjugates.[8] Unfortunately, most tumor cells have a much higher expression of Sia comparing to Gal or Fuc,[9] which works as a protective mechanism to resist the immune recognition and further weaken the immune stimulation during the immune-killing process. Thus, a glycan-transformation of the Sia on tumor cells to Gal or Fuc can simultaneously enhance the immune recognition and stimulation, which may be a most effective route from the aspects of glycans to improve immunotherapy of tumors.

Currently, methods by the blockage or cleavage of Sia on tumor cells to weaken immune escape have been widely developed.[10–13] They usually utilize inhibitors to inhibit the activities of intracellular sialyltransferase or sialidase to directly cleave the Sia on tumor cells.[14–16] On the other hand, the introduction of Gal or Fuc terminated glycoconjugates by lipophilicity-mediated membrane fusion to enhance immune stimulation are also popular.[14] However, the inhibitors often need a long time to work, and the glycosidases are fragile in the biological environment. Besides, whether the glycosidase-mediated cleavage or lipophilicity-mediated introduction suffer from the long processing time and the low glycan-transformation efficiency, which finally lead to limited enhancement of the immune-killing. Therefore, rapid blockage or cleavage of Sia and huge introduction of Gal or Fuc, preferably simultaneous, can extremely enhance the efficacy of immune-killing.

Herein, this work designs an ultra-galactocation to Sia strategy by using a penta-functional dendritic probe (Den@5F), which simultaneously achieves rapid blockage of Sia and huge introduction of Gal on tumor cell in vivo, leading to an efficient enhancement of the immune-killing of tumor cells. The Den@5F is conveniently constructed on a bis-MPA-acetylene dendrimer (Den-Acet) through a two-step reaction, which is firstly conjugated with azide labeled Gal (Gal–PEG–$N_3$), amino ($H_2N$–PEG–$N_3$) and Cy5 (Cy5–$N_3$) through the click reactions (Figure 1a).[17,18] The obtained Den@Gal/Cy5/$NH_2$ is further conjugated with carboxyphenylboronic acid (HOOC–PBA) and methyl 4-(4-(hydroxymethyl)-2-methoxy-5-nitrophenoxy) butanoate (mNB) with excessive amino groups through amide condensations[19,20] to obtain the Den@Gal/Cy5/$NH_2$/PBA/mNB, i.e. Den@5F. After subcutaneous injection of Den@5F into the tumor periphery of the tumor-bearing mouse, the highly expressed Sia on tumor cells is bound with Den@5F through the specific recognition between PBA and Sia (Figure 1b).[21–23] Under a subsequently UV radiation with a harmless dose on the tumor region,[24,25] the excessive Den@5Fs can multiply conjugate to the Den@5Fs bound on Sia through the photo-crosslinking between mNB and amino groups,[26,27] which achieves the ultra-galactocation to Sia on tumor cells. Due to the dendritic structure of the Den@5F,

[*] Y. Yang,[+] Y. Li,[+] C. Wang, Y. Wang, Y. Ren, Dr. J. Wu, Prof. Dr. H. Ju, Dr. Y. Chen
State Key Laboratory of Analytical Chemistry for Life Science, School of Chemistry and Chemical Engineering, Nanjing University Nanjing 210023 (P.R. China)
E-mail: hxju@nju.edu.cn
ylc@nju.edu.cn

[+] These authors contributed equally to this work.



© 2024 Wiley-VCH GmbH

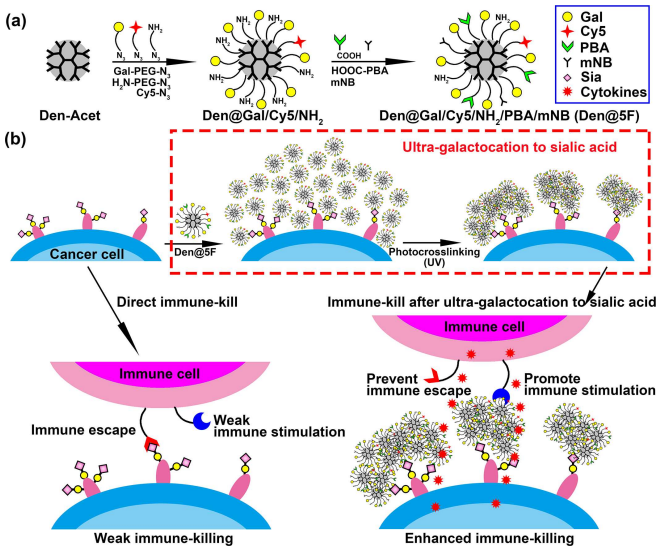


***Figure 1.*** Schematic illustration of the (a) preparation of Den@5F and (b) ultra-galactocation to sialic acid on tumor cells with Den@5F for enhanced immune-killing.

the comprehensively blocked Sia and hugely introduced Gal on tumor cells can simultaneously prevent the immune escape and promote the immune stimulation of the immune cells, which lead to the efficient enhancement of the immune-killing of tumor cells. For the proof of concept, the human breast cancer MCF-7 cells, mouse breast cancer 4T1 cells xenografted mice and the human natural killer (NK-92) cells are used as the models. The designed strategy successfully achieves enhanced immune-killing of tumor cells in vitro and the efficient tumor suppressions in vivo on tumor-bearing mice, which demonstrates the great potential of this ultra-galactocation to Sia strategy for the clinical applications of tumor immunotherapy.

Gal–PEG–$N_3$ was obtained by the deacetylation of the commercial 4AcGal–PEG–$N_3$ using MtONa[25,28] (Figure S1a), which was proved by the obvious variation of the m/z value from 528.05 to 360.05 in ESI-MS analysis (Figure S1b,c). The mNB was synthesized following the previous report,[27] which exhibited correct NMR and MS spectrum (Figure S2). Den-Acet of generation 5 was chosen as the substrate of the probe, which contains 96 surface acetylene groups (Figure S3a). Gal–PEG–$N_3$, $H_2N$–PEG–$N_3$ and Cy5–$N_3$ was mixed with Den-Acet with a concentration ratio of 5:4:1:0.1 to obtain Den@Gal/Cy5/$NH_2$ through copper-catalyzed click reaction, which introduced abundant Gal for ultra-galactocation and enough amino groups for the followed modification of PBA and mNB. Subsequently, HOOC–PBA and mNB was mixed with Den@Gal/Cy5/$NH_2$ with a concentration ratio of 1:2:0.1 to obtain Den@5F through N-(3-dimethylaminopropyl)-N′-ethyl carbodiimide hydrochloride (EDC) and N-hydroxysuccinimide (NHS) assisted amide linkage,[26,29,30] which reserved excess amino groups on Den@5F for the photo-crosslinking with mNB. The residual copper in the Den@5Fs was evaluated by the EDS elemental mapping through HAADF-STEM imaging (Figure S4a). Comparing to the Den@5F additionally mixed with 2 mM $CuSO_4$, the residual copper in the final Den@5F was negligible, which promised the biosafety of the Den@5F. The control dendritic probes (Den@Cy5/$NH_2$/PBA/mNB, Den@Gal/Cy5/$NH_2$/PBA, Den@Gal/Cy5/$NH_2$/mNB) (Figure S3b) were prepared by replace the corresponding functional groups with 8-azido-3,6-dioxaoctanol (HO–PEG–$N_3$) or acetic acid. The conjugation of Cy5–$N_3$ on Den@Gal/Cy5/$NH_2$ and the subsequent Den@5F could be directly visualized by the obvious color difference of the solutions, which exhibited dark blue and fluorescence peaks around 670 nm for Den@Gal/Cy5/$NH_2$ and Den@5F (Figure S5), demonstrating the successful conjugation of Cy5 on the corresponding dendritic probes.

To verify the Gal on Den@5F, an amino modified polystyrene amino microsphere (PSM–$NH_2$) was coated with glutaraldehyde, which was further immobilized with soybean agglutinin (SBA) to obtain the PSM-SBA (Figure S6a). The successful immobilization of SBA on PSM was demonstrated by immobilizing the FITC conjugated SBA (FSBA) with the same procedure, which exhibited obvious FITC fluorescence around the PSM surface in confocal laser scanning microscope (CLSM) images comparing to the initial PSM–$NH_2$ (Figure S6b and c). The PSM-SBA was respectively incubated with Den@Cy5/$NH_2$, Den@Gal/Cy5/$NH_2$, Den@Cy5/$NH_2$/PBA/mNB, and Den@5F at 37 °C for 30 min, which were washed by PBS for three times and subjected to CLSM imaging. Obvious Cy5 fluorescence was observed on the Den@Gal/Cy5/$NH_2$ and Den@5F incubated PSM-SBA, while these on Den@Cy5/$NH_2$ and Den@Cy5/$NH_2$/PBA/mNB incubated PSM-SBA were negligible (Figure 2a), demonstrating the successful conjugation of Gal on the corresponding dendritic probes. To verify the mNB on Den@5F, PSM–$NH_2$ was respectively incubated with Den@Gal/Cy5/$NH_2$, Den@Gal/Cy5/$NH_2$/PBA, Den@Gal/Cy5/$NH_2$/mNB, and Den@5F at 37 °C for 10 min under UV radiation, which were washed by PBS for three times and subjected to CLSM imaging. Obvious Cy5 fluorescence was observed on the Den@Gal/Cy5/$NH_2$/mNB and Den@5F incubated PSM–$NH_2$, while these on Den@Gal/Cy5/$NH_2$ and Den@Gal/Cy5/$NH_2$/PBA incubated PSM-SBA were weak (Figure 2b), demonstrating the successful conjugation of mNB on the corresponding dendritic probes. The TEM images of Den@5Fs after UV radiation also exhibited a cross-linked morphology comparing to these without UV radiation (Figure S4b), which further demonstrated the mNB and amino groups mediated photo-crosslinking of Den@5Fs. The conjugation of PBA was demonstrated by incubating the MCF-7 cells with Den@Gal/Cy5/$NH_2$, Den@Cy5/$NH_2$/PBA, Den@5F at 37 °C for 30 min, respectively. An extra cell sample was incubated with Den@5F under UV radiation. After washed by PBS for three times and subjecting to CLSM imaging, obvious Cy5 fluorescence was observed on the Den@Cy5/$NH_2$/PBA, Den@5F incubated cells, while these on Den@Gal/Cy5/$NH_2$ incubated cells was negligible (Figure 2c), demonstrating the successful conjugation of PBA on the corresponding dendritic probes. The similar binding levels of Den@Gal/Cy5/$NH_2$/PBA and Den@5F to cells without UV radiation indicated the


© 2024 Wiley-VCH GmbH

15213757, 0, Downloaded from https://onlinelibrary.wiley.com/doi/10.1002/ange.202319849 by Nanjing University, Wiley Online Library on [10/04/2024]. See the Terms and Conditions (https://onlinelibrary.wiley.com/terms-and-conditions) on Wiley Online Library for rules of use; OA articles are governed by the applicable Creative Commons License

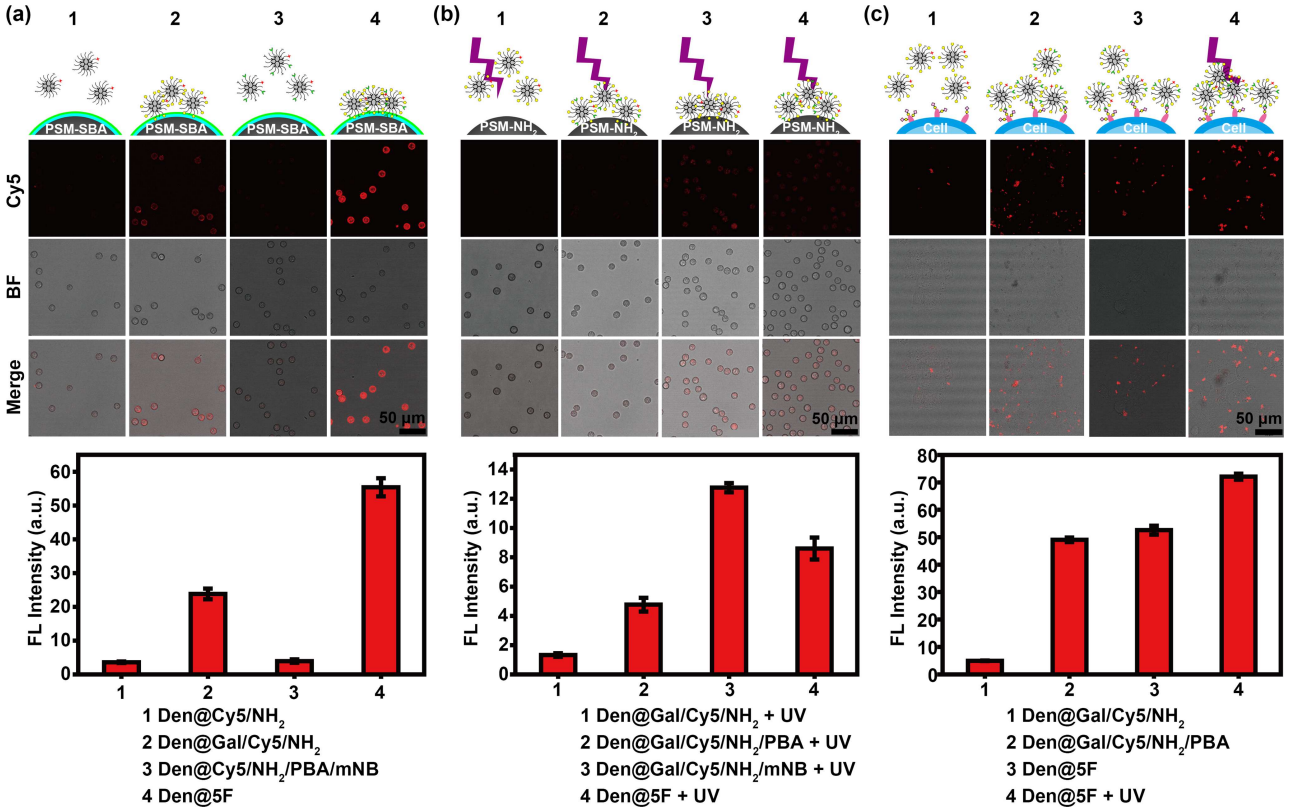


***Figure 2.*** (a) Schematic illustration, CLSM images and the statistical Cy5 fluorescence intensities of PSM-SBA microspheres incubated with (1) Den@Cy5/$NH_2$, (2) Den@Gal/Cy5/$NH_2$, (3) Den@Cy5/$NH_2$/PBA/mNB, and (4) Den@5F, respectively. (b) Schematic illustration, CLSM images and the statistical Cy5 fluorescence intensities of PSM- $NH_2$ microspheres incubated with (1) Den@Cy5/$NH_2$ under UV radiation, (2) Den@Gal/Cy5/$NH_2$/PBA under UV radiation, (3) Den@Cy5/$NH_2$/mNB under UV radiation, and (4) Den@5F under UV radiation, respectively. (c) Schematic illustration, CLSM images and the statistical Cy5 fluorescence intensities of MCF-7 cells incubated with (1) Den@Gal/Cy5/$NH_2$, (2) Den@Gal/Cy5/$NH_2$/PBA, (3) Den@5F, and (4) Den@5F under UV radiation, respectively. Scale bar, 50 μm. The error bars indicate mean ± SD ($n = 3$).

negligible influence of mNB without UV during the probe-cell bindings. Besides, the cells incubated with Den@5F under UV radiation exhibited a higher Cy5 fluorescence intensity comparing to those without UV radiation, which further demonstrated the mNB mediated photo-crosslinking to introduce more Den@5Fs on cells. Thus, the designed Den@5F could successfully achieve ultra-galactocation to Sia on cell surface through mNB mediated photo-cross-linking of excessive Den@5Fs.

To investigate the enhancement of the immune-killing ability of the designed strategy, MCF-7 cells were respectively incubated with Den@Gal/Cy5/$NH_2$/PBA, Den@Cy5/$NH_2$/PBA/mNB and Den@5F at 37 °C for 30 min and radiated by UV for another 10 min. Subsequently, the dendritic probes bound cells were incubated with NK-92 cells for 2, 4, 8, 12 h, and then stained with calcein-AM/propidium iodide (PI) to collect CLSM images (Figure 3). The cells without dendritic probes but UV radiation exhibited tiny variation of the calcein-AM fluorescence and negligible PI fluorescence, indicating the harmless dose of UV radiation. The Den@Cy5/$NH_2$/PBA/mNB treated cells exhibited a decrease of calcein-AM fluorescence and an increase of PI fluorescence after incubated with NK-92 cells for 8 h, which indicated the Sia blockage induced enhancement of immune-killing. In contrast, the Den@Gal/Cy5/$NH_2$/PBA and Den@5F exhibited obvious decreases of calcein-AM fluorescence and increases of PI fluorescence within 4 h, while the latter exhibited an obvious immune-killing of the tumor cells shortly after 2 h. As negative controls, the dendritic probes bound cells without NK-92 cells treatment exhibited strong calcein-AM fluorescence and invisible PI fluorescence after 24 h (Figure S7), indicating the negligible toxicity of the dendritic probes themselves. It could be indicated that the combination of the Sia blockage and Gal introduction could further enhance the immune-killing, while a multiple Gal introduction through photo-crosslinking could maximumly prevent the immune escape and promote the immune stimulation of the immune cells in the aspect of glycans, which lead to the rapid and efficient immune-killing of tumor cells.

To demonstrate the enhanced immune-killing of the designed dendritic probes, six groups of 4T1 subcutaneous tumor xenograft mice with tumor volume of ~100 $mm^3$ were received injections of saline, saline with UV radiation, Den@Cy5/$NH_2$/PBA/mNB with UV radiation, Den@Gal/Cy5/$NH_2$/PBA, Den@5F and Den@5F with UV radiation at tumor periphery every other day for 15 days, respectively (Figure 4a). As the thickness of the mouse skin was around


© 2024 Wiley-VCH GmbH

15213757, 0, Downloaded from https://onlinelibrary.wiley.com/doi/10.1002/ange.202319849 by Nanjing University, Wiley Online Library on [10/04/2024]. See the Terms and Conditions (https://onlinelibrary.wiley.com/terms-and-conditions) on Wiley Online Library for rules of use; OA articles are governed by the applicable Creative Commons License

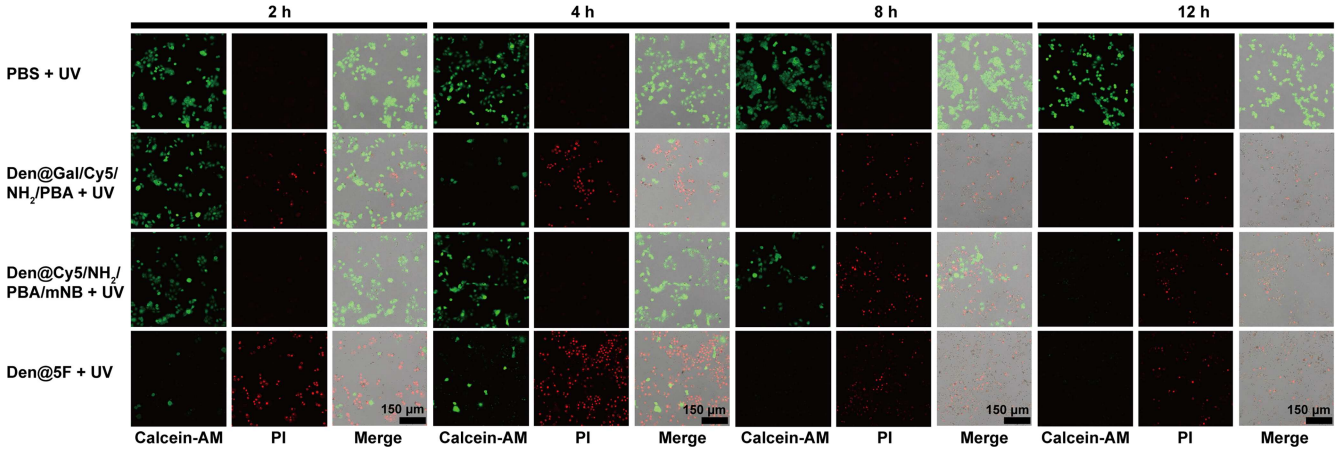


***Figure 3.*** CLSM images of MCF-7 cells respectively incubated with PBS, Den@Gal/Cy5/$NH_2$/PBA, Den@Cy5/$NH_2$/PBA/mNB and Den@5F at 37 °C for 30 min with a subsequent UV radiation for 10 min, and then with NK-92 cells for 2, 4, 8, or 12 h, which were finally all stained with calcein-AM/PI. Scale bar, 150 μm.

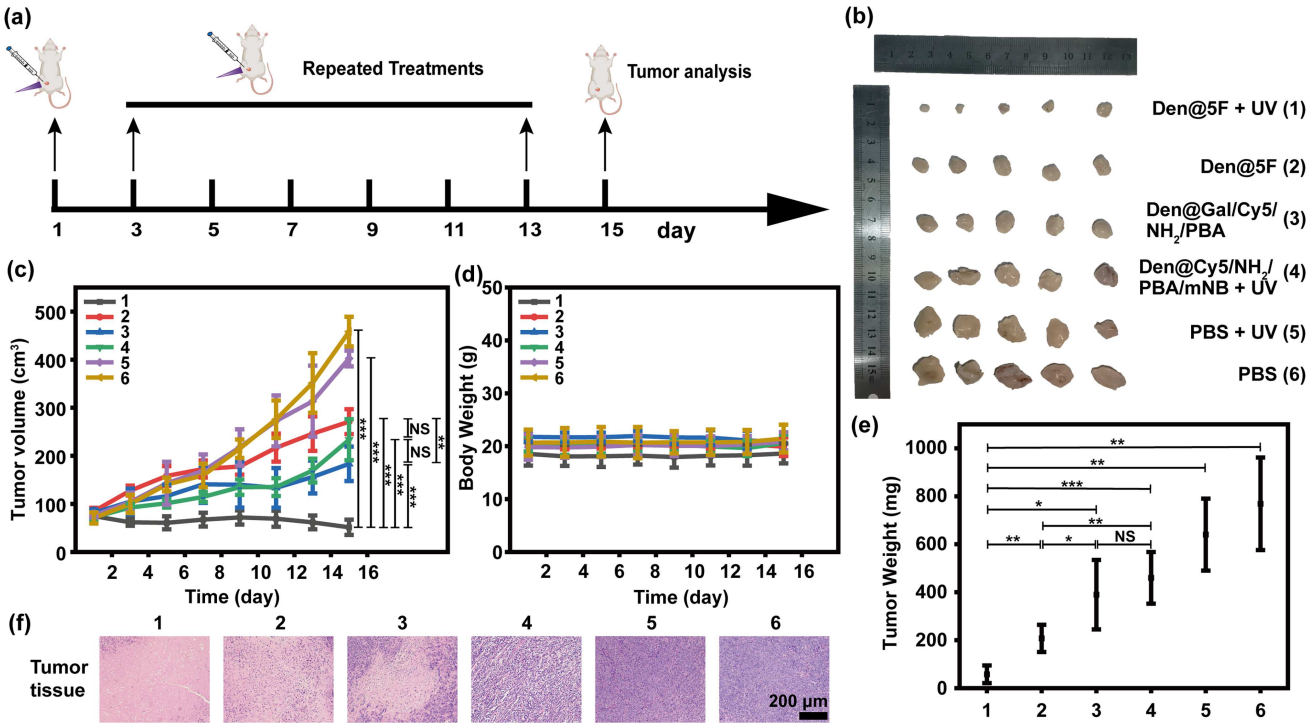


***Figure 4.*** (a) Schematic illustration for the treatment of 4T1 tumor-bearing mice with seven repeated injections on day 1, 3, 5, 7, 9, 11 and 13. (b) Photographs of tumor tissues dissected from 4T1 tumor-bearing mice after treated with (1) Den@5F with UV radiation, (2) Den@5F, (3) Den@Gal/Cy5/$NH_2$/PBA, (4) Den@Cy5/$NH_2$/PBA/mNB with UV radiation, (5) saline with UV radiation, and (6) saline. (c,d,e) Variation of tumor volume (c) body weight (d), and tumor weight (e) of 4T1 tumor-bearing mice after treated with (1) to (6). (f) Histology images of sectioned tumor tissues after H&E staining. Scale bar, 200 μm. The error bars indicate mean ± SD ($n = 5$). Statistical analysis was performed by unpaired two-tailed t-tests (*$p < 0.05$; **$p < 0.005$; ***$p < 0.0005$; NS, not significant), $n = 5$.

200 μm,[31,32] the 365 nm UV light with a skin penetrating depth of 800 μm[33–35] can efficiently radiate the dendritic probes in the tumors. The UV radiation was performed after 30 min of each injection and lasting 10 min. The body weight of all mice did not exhibit discernible difference during the treatment (Figure 4d), and no pathological abnormalities was observed in their heart, liver, spleen, lung and kidney (Figure S8), indicating the negligible side effects under these treatments. The retention of the dendritic probes in the tumor region of mice was investigated by in vivo mice imaging at 0.5–48 h after injection. Comparing to the mice treated with Den@Gal/Cy5/$NH_2$/PBA, the mice treated with Den@5F exhibited a stronger Cy5 fluorescence at the tumor region within 48 h, which exhibited an enhanced retention of


© 2024 Wiley-VCH GmbH

15213757, 0, Downloaded from https://onlinelibrary.wiley.com/doi/10.1002/ange.202319849 by Nanjing University, Wiley Online Library on [10/04/2024]. See the Terms and Conditions (https://onlinelibrary.wiley.com/terms-and-conditions) on Wiley Online Library for rules of use; OA articles are governed by the applicable Creative Commons License

the probes at 48 h after UV radiation (Figure S9). After treated for 15 days, the tumor volume and weight of the mice treated with dendritic probes exhibited obvious inhibition comparing to these treated with saline or saline with UV radiation (Figure 4b,c,e). The mice treated with Den@Cy5/$NH_2$/PBA/mNB with UV radiation, Den@Gal/Cy5/$NH_2$/PBA, Den@5F exhibited a certain inhibition of the tumor volume and weight, which could be attributed to the Sia blockage or Gal introduction enhanced immune-killing. The mice treated with Den@5F and UV radiation exhibited the minimum tumor volume and weight, indicating the strongest enhancement of immune-killing among these groups by the simultaneous Sia blockage and huge Gal introduction. The pathological states of tumor tissues dissected from each treated group were assessed by hematoxylin and eosin (H&E) assay. The tissue from Den@5F and UV radiation treated mouse exhibited the largest necrotic area comparing to all the other groups (Figure 4f), which was consistent to the changes of tumor volume and weight. To further validate the simultaneous Sia blockage and huge Gal introduction of Den@5F and UV radiation treatment in in vivo immune-killing, the tumor tissues dissected from each treated group were respectively stained with FITC-SBA and FITC-SNA (Figure S10). The tissue slices from the mice treated with Den@Cy5/$NH_2$/PBA/mNB with UV radiation, Den@Gal/Cy5/$NH_2$/PBA, Den@5F and Den@5F with UV radiation exhibited significant decrease of FITC-SNA fluorescence comparing to these from PBS treated mice, indicating the successful blockage of Sia by these dendritic probes in vivo. Meanwhile, the tissue slices from the mice treated with Den@Gal/Cy5/$NH_2$/PBA, Den@5F exhibited obviously increase of the FITC-SBA fluorescence comparing to these from PBS and Den@Cy5/$NH_2$/PBA/mNB with UV radiation treated mice, indicating the successful introduction of Gal to the tumor cell surface in vivo. Besides, the tissue slices from the mice treated with Den@5F and UV radiation exhibited a strongest FITC-SBA fluorescence, indicating the successful ultra-galactocation by photo-crosslinking in vivo. Thus, the ultra-galactocation to Sia on tumor cell surface could exactly achieve maximum enhancement of in vivo immune-killing from the aspects of glycans.

In conclusion, this work proposes an ultra-galactocation to Sia strategy by using a Den@5F probe to comprehensively block Sia and hugely introduce Gal simultaneously on tumor cells in vivo, which efficiently enhance the immune-killing of tumor cells. The Den@5F can be conveniently prepared by conjugating five different kinds of functional groups to a dendrimer through a two-step reaction, which achieves maximum enhancement of in vivo immune-killing from the aspects of glycans. Although the limited penetration of UV radiation may constrain certain clinical applications of this strategy, it can be probably solved by the use of optical fibers. By simply changing the corresponding components on the dendritic probes, the proposed strategy can theoretically be extended for simultaneous blockage and introduction of various different functional molecules in vivo, providing a significant and promising tool to promote the clinical immunotherapy of tumors.

## Acknowledgements

This work was financially supported by National Natural Science Foundation of China (21974063, 21827812 and 21890741).

## Conflict of Interest

The authors declare no conflict of interest.

## Data Availability Statement

The data that support the findings of this study are available from the corresponding author upon reasonable request.

**Keywords:** Immune-killing · Tumor · Galactose · Sialic acid · Dendrimer

[1] A. Varki, *Glycobiology* **2017**, *27*, 3–49.
[2] Y. Dong, W. Li, Z. Gu, R. Xing, Y. Ma, Q. Zhang, Z. Liu, *Angew. Chem. Int. Ed.* **2019**, *58*, 10621–10625.
[3] S. Hong, C. Yu, P. Wang, Y. Shi, W. Cao, B. Cheng, D. G. Chapla, Y. Ma, J. Li, E. Rodrigues, Y. Narimatsu, J. R. Yates, X. Chen, H. Clausen, K. W. Moremen, M. S. Macauley, J. C. Paulson, P. Wu, *Angew. Chem. Int. Ed.* **2020**, *60*, 3603–3610.
[4] A. L. Parry, N. A. Clemson, J. Ellis, S. S. Bernhard, B. G. Davis, N. R. Cameron, *J. Am. Chem. Soc.* **2013**, *135*, 9362–9365.
[5] S. Hong, C. Yu, P. Wang, Y. Shi, W. Cao, B. Cheng, D. G. Chapla, Y. Ma, J. Li, E. Rodrigues, Y. Narimatsu, J. R. Yates, X. Chen, H. Clausen, K. W. Moremen, M. S. Macauley, J. C. Paulson, P. Wu, *Angew. Chem. Int. Ed.* **2020**, *60*, 3603–3610.
[6] C. Pifferi, R. Fuentes, A. Fernández-Tejada, *Nat. Chem. Rev.* **2021**, *5*, 197.
[7] E. RodrÍguez, S. T. T. Schetters, Y. van Kooyk, *Nat. Rev. Immunol.* **2018**, *18*, 204.
[8] S. Julien, P. A. Videira, P. Delannoy, *Biomol. Eng.* **2012**, *2*, 435–466.
[9] S. S. Pinho, C. A. Reis, *Nat. Rev. Cancer* **2015**, *15*, 540–555.
[10] H. Xiao, E. C. Woods, P. Vukojicic, C. R. Bertozzi, *Proc. Natl. Acad. Sci. USA* **2016**, *113*, 10304–10309.
[11] M. A. Gray, M. A. Stanczak, N. R. Mantuano, H. Xiao, J. F. A. Pijnenborg, S. A. Malaker, C. L. Miller, P. A. Weidenbacher, J. T. Tanzo, G. Ahn, E. C. Woods, H. Läubli, C. R. Bertozzi, *Nat. Chem. Biol.* **2020**, *16*, 1376–1384.
[12] H.-H. Lee, Y.-N. Wang, W. Xia, C.-H. Chen, K.-M. Rau, L. Ye, Y. Wei, C.-K. Chou, S.-C. Wang, M. Yan, C.-Y. Tu, T.-C. Hsia, S.-F. Chiang, K. S. C. Chao, I. I. Wistuba, J. L. Hsu, G. N. Hortobagyi, M.-C. Hung, *Cancer Cell* **2019**, *36*, 168–178.
[13] C. Büll, T. J. Boltje, N. Balneger, S. M. Weischer, M. Wassink, J. J. van Gemst, V. R. Bloemendal, L. Boon, J. van der Vlag, T. Heise, M. H. den Brok, G. J. Adema, *Cancer Res.* **2018**, *78*, 3574–3588.
[14] C. Zheng, Q. Zhong, W. Song, K. Yi, H. Kong, H. Wang, Y. Tao, M. Li, X. Chen, *Adv. Mater.* **2023**, *35*, 2206989.
[15] M. Okada, S. Chikuma, T. Kondo, S. Hibino, H. Machiyama, T. Yokosuka, M. Nakano, A. Yoshimura, *Cell Rep.* **2017**, *20*, 1017–1028.
[16] C. Büll, T. J. Boltje, M. Wassink, A. M. A. de Graaf, F. L. van Delft, M. H. den Brok, G. J. Adema, *Mol. Cancer Ther.* **2013**, *12*, 1935–1946.


© 2024 Wiley-VCH GmbH

15213757, 0, Downloaded from https://onlinelibrary.wiley.com/doi/10.1002/ange.202319849 by Nanjing University, Wiley Online Library on [10/04/2024]. See the Terms and Conditions (https://onlinelibrary.wiley.com/terms-and-conditions) on Wiley Online Library for rules of use; OA articles are governed by the applicable Creative Commons License

[17] V. V. Rostovtsev, L. G. Green, V. V. Fokin, K. B. Sharpless, *Angew. Chem. Int. Ed.* **2002**, *41*, 2596–2599.
[18] C. W. Tornøe, C. Christensen, M. Meldal, *J. Org. Chem.* **2002**, *67*, 3057–3064.
[19] V. R. Pattabiraman, J. W. Bode, *Nature* **2011**, *480*, 471–479.
[20] A. Leggio, J. Bagalà, E. L. Belsito, A. Comandè, M. Greco, A. Liguori, *Chem. Cent. J.* **2017**, *11*, 87.
[21] A. Matsumoto, H. Cabral, N. Sato, K. Kataoka, Y. Miyahara, *Angew. Chem. Int. Ed.* **2010**, *49*, 5494–5497.
[22] A. Matsumoto, N. Sato, K. Kataoka, Y. Miyahara, *J. Am. Chem. Soc.* **2009**, *131*, 12022–12023.
[23] H. Otsuka, E. Uchimura, H. Koshino, T. Okano, K. Kataoka, *J. Am. Chem. Soc.* **2003**, *125*, 3493–3502.
[24] D. Wang, S. Du, A. Cazenave-Gassiot, J. Ge, J.-S. Lee, M. R. Wenk, S. Q. Yao, *Angew. Chem. Int. Ed.* **2017**, *56*, 5829–5833.
[25] N. Kong, J. Zhou, J. Park, S. Xie, O. Ramström, M. Yan, *Anal. Chem.* **2015**, *87*, 9451–9458.
[26] Y. Yang, J. Zhang, Z. Liu, Q. Lin, X. Liu, C. Bao, Y. Wang, L. Zhu, *Adv. Mater.* **2016**, *28*, 2724–2730.
[27] T. Pauloehrl, G. Delaittre, M. Bruns, M. Meißler, H. G. Börner, M. Bastmeyer, C. Barner-Kowollik, *Angew. Chem. Int. Ed.* **2012**, *51*, 9181–9184.
[28] O. Michel, B. J. Ravoo, *Langmuir* **2008**, *24*, 12116–12118.
[29] J. Hua, Z. Li, W. Xia, N. Yang, J. Gong, J. Zhang, C. Qiao, *Mater. Sci. Eng. C* **2016**, *61*, 879–892.
[30] M. J. E. Fischer, *Methods Mol. Biol.* **2010**, *627*, 55–73.
[31] C. P. Sabino, A. M. Deana, T. M. Yoshimura, D. F. T. da Silva, C. M. França, M. R. Hamblin, M. S. Ribeiroa, *J. Photochem. Photobiol. B* **2016**,*160*, 72–78.
[32] J. C. J. Wei, G. A. Edwards, D. J. Martin, H. Huang, M. L. Crichton, M. A. F. Kendall, *Sci. Rep.* **2017**, *7*, 15885.
[33] E. Ruggiero, S. A. Castro, A. Habtemariam, L. Salassa, *Dalton Trans.* **2016**, *45*, 13012–13020.
[34] C. Ash, M. Dubec, K. Donne, T. Bashford, *Lasers Med. Sci.* **2017**, *32*, 1909–1918.
[35] L. Finlayson, I. R. M. Barnard, L. McMillan, S. H. Ibbotson, C. T. A. Brown, E. Eadie, K. Wood, *Photochem. Photobiol.* **2022**, *98*, 974–981.

Manuscript received: December 21, 2023
Accepted manuscript online: March 4, 2024
Version of record online: ■■, ■■


© 2024 Wiley-VCH GmbH

15213757, 0, Downloaded from https://onlinelibrary.wiley.com/doi/10.1002/ange.202319849 by Nanjing University, Wiley Online Library on [10/04/2024]. See the Terms and Conditions (https://onlinelibrary.wiley.com/terms-and-conditions) on Wiley Online Library for rules of use; OA articles are governed by the applicable Creative Commons License

# Zuschriften

**Immunotherapy**

Y. Yang, Y. Li, C. Wang, Y. Wang, Y. Ren, J. Wu, H. Ju,* Y. Chen* —— **e202319849**

Ultra-Galactocation to Sialic Acid on Tumor Cells with A Penta-Functional Dendritic Probe for Enhanced Immune-Killing

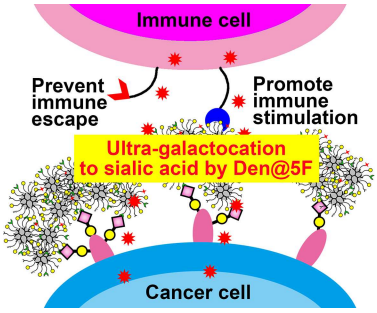


Enhance immune-killing: A ultra-galactocation to sialic acid strategy is designed by using a penta-functional dendritic probe (Den@5F) to simultaneously block sialic acid and hugely introduce galactose on tumor cells in vivo for the enhancement of immune-killing.



© 2024 Wiley-VCH GmbH

15213757, 0, Downloaded from https://onlinelibrary.wiley.com/doi/10.1002/ange.202319849 by Nanjing University, Wiley Online Library on [10/04/2024]. See the Terms and Conditions (https://onlinelibrary.wiley.com/terms-and-conditions) on Wiley Online Library for rules of use; OA articles are governed by the applicable Creative Commons License